

Article

## Origins of Selectivity for the [2+2] Cycloaddition of $\alpha,\beta$ -unsaturated Ketones within a Porous Self-assembled Organic Framework

Jun Yang, Mahender B. Dewal, Salvatore Profeta,, Mark D. Smith, Youyong Li, and Linda S. Shimizu

*J. Am. Chem. Soc.*, **2008**, 130 (2), 612-621 • DOI: 10.1021/ja076001+

Downloaded from <http://pubs.acs.org> on February 8, 2009

### More About This Article

Additional resources and features associated with this article are available within the HTML version:

- Supporting Information
- Links to the 3 articles that cite this article, as of the time of this article download
- Access to high resolution figures
- Links to articles and content related to this article
- Copyright permission to reproduce figures and/or text from this article

[View the Full Text HTML](#)



**ACS Publications**  
High quality. High impact.

## Origins of Selectivity for the [2+2] Cycloaddition of $\alpha,\beta$ -unsaturated Ketones within a Porous Self-assembled Organic Framework

Jun Yang,<sup>†</sup> Mahender B. Dewal,<sup>†</sup> Salvatore Profeta, Jr.,<sup>†</sup> Mark D. Smith,<sup>†</sup>  
Youyong Li,<sup>‡</sup> and Linda S. Shimizu\*<sup>†</sup>

Department of Chemistry and Biochemistry, University of South Carolina, Columbia,  
South Carolina 29208, Materials and Process Simulation Center,  
California Institute of Technology, California 91125

Received August 9, 2007; E-mail: shimizul@mail.chem.sc.edu

**Abstract:** This article studies the origins of selectivity for the [2+2] cycloadditions of  $\alpha,\beta$ -unsaturated ketones within a porous crystalline host. The host, formed by the self-assembly of a bis-urea macrocycle, contains accessible channels of  $\sim 6$  Å diameter and forms stable inclusion complexes with a variety of cyclic and acyclic  $\alpha,\beta$ -unsaturated ketone derivatives. Host 1 crystals provide a robust confined reaction environment for the highly selective [2+2] cycloaddition of 3-methyl-2-cyclopentenone, 2-cyclohexenone, and 2-methyl-2-cyclopentenone, forming their respective exo head-to-tail dimers in high conversion. The products are readily extracted from the self-assembled host and the crystalline host can be efficiently recovered and reused. Molecular modeling studies indicate that the origin of the observed selectivity is due to the excellent match between the size and shape of these guests to dimensions of the host channel and to the preorganization of neighboring enones into favorable reaction geometries. Small substrates, such as acrylic acid and methylvinylketone, were bound by the host and were protected from photoreactions. Larger substrates, such as 4,4-dimethyl-2-cyclohexenone and mesityl oxide, do not undergo selective [2+2] cycloaddition reactions. In an effort to understand these differences in reactivity, we examined these host-guest complexes by thermogravimetric analysis (TGA), NMR, powder X-ray diffraction (PXRD) and molecular modeling.

### Introduction

There is great interest in developing synthetic hosts that possess the extraordinary efficiency and specificity of enzymes.<sup>1</sup> A number of groups have designed and synthesized hollow host molecules<sup>2,3</sup> to facilitate the reaction of encapsulated guests. Others have explored the use of porous materials as confined

reaction environments.<sup>4</sup> Often, the reactions inside these designed environments proceed at enhanced rates and exhibit unusual selectivity,<sup>1a</sup> which is generally attributed to entropic effects.<sup>5</sup> Molecular hosts, though often challenging to synthesize, allow exquisite control of the cavity dimensions and properties that may translate into control of the reaction geometry and selectivity. Conversely, porous materials, such as zeolites,<sup>6</sup> mesoporous silica,<sup>7</sup> and coordination polymers<sup>8</sup> are readily

<sup>†</sup> University of South Carolina.

<sup>‡</sup> California Institute of Technology.

- (1) (a) Vriezema, D. M.; Aragones, M. C.; Elemans, J. A. A. W.; Cornelissen, J. J. L. M.; Rowan, A. E.; Nolte, R. J. M. *Chem. Rev.* **2005**, *105*, 1445–1489. (b) Kirby, A. J. *Angew. Chem., Int. Ed. Engl.* **1996**, *35*, 707–24. (2) (a) Natarajan, A.; Kaanumalle, L. S.; Jockusch, S.; Gibb, C. L. D.; Gibb, B. C.; Turro, N. J.; Ramamurthy, V. *J. Am. Chem. Soc.* **2007**, *129*, 4132–4133. (b) Rebek, J. J. *Angew. Chem., Int. Ed.* **2005**, *44*, 2068–2078. (c) Kang, J.; Rebek, J., Jr. *Nature* **1997**, *385*, 50–52. (d) Takahashi, K. *Chem. Rev.* **1998**, *98*, 2013–2033. (e) Yoshizawa, M.; Fujita, M. *Pure Appl. Chem.* **2005**, *77*, 1107–1112. (f) Breslow, R.; Dong, S. D. *Chem. Rev.* **1998**, *98*, 1997–2011. (g) Marty, M.; Clyde-Watson, Z.; Twyman, L. J.; Nakash, M.; Sanders, J. K. M. *Chem. Comm.* **1998**, 2265–2266. (h) Nakash, M.; Sanders, J. K. M. *J. Org. Chem.* **2000**, *65*, 7266–7271. (i) Leung, D. H.; Fielder, D.; Bergman, R. G.; Raymond, K. N. *Ang. Chem. Int. Ed.* **2004**, *43*, 963–966. (j) Kang, Y.; Zyryanov, G. V.; Rudkevich, D. M. *Chem. Eur. J.* **2005**, *11*, 1924–1932. (k) Warmuth, R.; Makowiec, S. *J. Am. Chem. Soc.* **2005**, *127*, 1084–1085. (3) (a) Yoshizawa, M.; Fujita, M. *Pure Appl. Chem.* **2005**, *77*, 1107–1112. (b) Nishioka, Y.; Yamaguchi, T.; Yoshizawa, M. *J. Am. Chem. Soc.* **2007**, *129*, 7000–7001. (c) Karthikeyan, S.; Ramamurthy, V. *J. Org. Chem.* **2007**, *72*, 452–458. (d) Wu, C.-D.; Lin, W. *Angew. Chem., Int. Ed.* **2007**, *46*, 1075–1078. (e) Dybsteve, D. N.; Nuzhdin, A. L.; Chun, H.; Bryliakov, K. P.; Talsi, E. P.; Fedin, V. P.; Kim, K. *Angew. Chem., Int. Ed.* **2007**, *45*, 916–920.

- (4) (a) Turro, N. J. *Photochem. Photobiol. A* **1996**, *100*, 53–56. (b) Ramamurthy, V.; Eaton, D. F.; Caspar, J. V. *Acc. Chem. Res.* **1992**, *25*, 299–307. (c) Hashimoto, S. *J. Photochem. Photobiol., C* **2003**, *4*, 19–49. (d) Garcia, H.; Roth, H. D. *Chem. Rev.* **2002**, *102*, 3947–4007. (e) Tung, C. H.; Wu, L. Z.; Zhang, L. P.; Chen, B. *Acc. Chem. Res.* **2003**, *36*, 39–40. (f) Kaupp, G. *Top. Curr. Chem.* **2005**, *254*, 95–183. (g) MacGillivray, L. R.; Papaefstathiou, G. S.; Friscic, T.; Varshney, D. B.; Hamilton, T. D. *Top. Curr. Chem.* **2004**, *248*, 201–221. (h) Tanaka, K.; Mochizuki, E.; Yasui, N.; Kai, Y.; Miyahara, I.; Hirotsu, K.; Toda, F. *Tetrahedron* **2000**, *56*, 6853–6865. (i) Yoshizawa, M.; Takeyama, Y.; Okano, T.; Fujita, M. *J. Am. Chem. Soc.* **2003**, *125*, 3243–3247. (j) Madhavan, D.; Pitchumani, K. *Photochem. Photobiol. Sci.* **2002**, *1*, 991–995. (k) Usami, H.; Takagi, K.; Sawaki, Y. *Chem. Lett.* **1992**, 1405–1408. (5) Cacciapaglia, R.; Di Stefano, S.; Mandolini, L. *Acc. Chem. Res.* **2004**, *37*, 113–122. (6) (a) Tao, Y. S.; Kanoh, H.; Abrams, L.; Kaneko, K. *Chem. Rev.* **2006**, *106*, 896–910. (b) Cundy, C. S.; Cox, P. A. *Microporous Mesoporous Mater.* **2005**, *82*, 1–78. (7) Vinu, A.; Hossain, K. Z.; Ariga, K. *J. Nanosci. Nanotech.* **2005**, *5*, 347–371. (8) (a) Suslick, K. S.; Bhyrappa, P.; Chou, J. H.; Kosal, M. E.; Nakagaki, S.; Smithenry, D. W.; Wilson, S. R. *Acc. Chem. Res.* **2005**, *38*, 283–291. (b) Ockwig, N. W.; Delgado-Friedrichs, O.; O'Keefe, M.; Yaghi, O. M. *Acc. Chem. Res.* **2005**, *28*, 176–182.

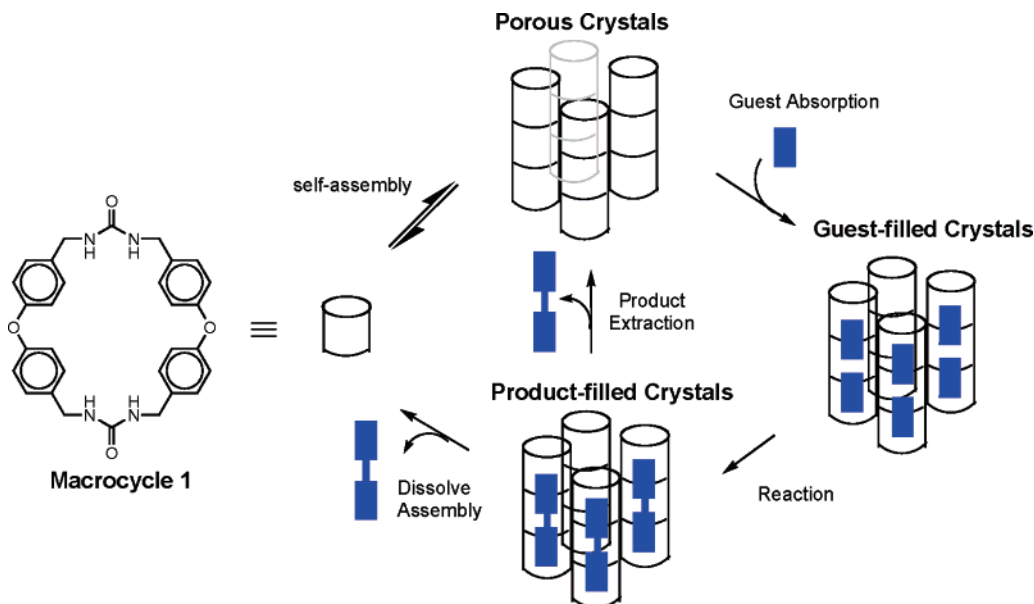


**Figure 1.** Schematic representation of the self-assembly of macrocycle **1** into crystalline host **1**, containing columnar channels. The porous crystals can reversibly absorb a variety of guests including 2-cyclohexenone. UV-irradiation of included guests yields a photodimer in high conversion and selectivity. The guests can be readily extracted from the crystals, and the crystals can be reused.

synthesized, but it is often more difficult to control and tailor their cavity dimensions and properties. We have taken a hybrid approach of using a rigid molecular host that self-assembles into a porous material. This hybrid approach allows for readily synthesizing large quantities of porous materials with well-defined channels of predetermined dimensions for use as confined reaction environments.

We have developed macrocyclic bis-urea **1** that stacks into columns, forming crystalline host **1** with guest accessible channels (Figure 1).<sup>9</sup> Crystalline host **1** can selectively bind guests<sup>10</sup> and facilitates the [2+2] cycloaddition of included 2-cyclohexenone to selectively yield the head-to-tail photodimer in high conversion.<sup>11</sup> Not only does host **1** induce a highly selective reaction, but it also allows the product to be easily isolated by extraction and facilitates efficient recovery of the crystalline host for reuse. We are interested in understanding the unique features of our system that lead to such high selectivity and conversion. Specifically, we will use a range of different  $\alpha,\beta$ -unsaturated ketones to probe the origins of the exclusive formation of the exo head-to-tail [2+2] product in high conversion. In addition, molecular modeling will be used to try to understand the reasons behind the observed products and to see if one can develop a predictable model for this system.

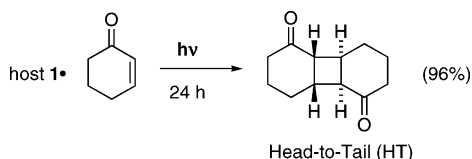
The [2+2] cycloaddition reaction was chosen because it is an excellent probe of the shape, symmetry, and homogeneity of our self-assembled reaction environment. The [2+2] cycloaddition reaction has proven to be a key transformation in the synthesis of a number of natural products and pharmaceuticals.<sup>12</sup> Therefore, the ability to better control the selectivity and efficiency of this reaction would enhance its synthetic utility. The [2+2] cycloaddition reactions are known to give a range

of products, and product distributions are very sensitive to the surrounding reaction environment.<sup>13</sup> The major products are the exo and endo head-to-tail (HT) and head-to-head (HH) products. These products are formed when two alkenes are brought together in a suprafacial orientation within 4.2 Å of each other.<sup>14</sup> Other minor products are also observed including ring opened dimers. In general, [2+2] cycloadditions of enones within a zeolite or on a surface can result in selectivity for either HT or the HH, depending on the individual enone structure. For example, the [2+2] cycloaddition of 2-cyclohexenone within a zeolite yields high selectivities for the HH product due to coordination to the carbonyl oxygen and to steric factors.<sup>4j,15</sup> Crystalline host **1** is unusual in two respects. First, it facilitates the [2+2] cycloadditions reaction with high conversion and high selectivity. Second, it yields selectively the exo HT dimer, in contrast to most previous host systems that favored the exo HH product.<sup>4,15</sup>

To investigate the origins of selectivity and also the utility of host **1** as a confined reaction environment, we examined a range of  $\alpha,\beta$ -unsaturated ketones in terms of size and shape. First, we examined the ability of the synthetic host framework to selectively absorb and release the reactants. These binding experiments were carried out by following the absorption and desorption, using TGA and NMR. Second, we examined the shape and symmetry of the host environment using powder X-ray diffraction and computer modeling. Third, we examined the product distribution and yields of the cycloaddition products. High selectivity and conversion was observed for the medium sized enones because they were complementary to the reaction

(9) (a) Shimizu, L. S.; Hughes, A. D.; Smith, M. D.; Davis, M. J.; Zhang, B. P.; Zur Loye, H. C.; Shimizu, K. D. *J. Am. Chem. Soc.* **2003**, *125*, 14972–14973. (b) Shimizu, L. S.; Hughes, A. D.; Smith, M. D.; Samuel, S. A.; Ciurtin-Smith, D. *Supramol. Chem.* **2005**, *17*, 27–30.  
 (10) Dewal, M. B.; Lufaso, M. W.; Hughes, A. D.; Samuel, S. A.; Pellechia, P.; Shimizu, L. S. *Chem. Mater.* **2006**, *18*, 4855–4864.  
 (11) Yang, J.; Dewal, M. B.; Shimizu, L. S. *J. Am. Chem. Soc.* **2006**, *128*, 8122–8123.

(12) (a) Mascitti, V.; Corey, E. J. *J. Am. Chem. Soc.* **2006**, *128*, 3118–3119. (b) Iriondo-Alberdi, J.; Greaney, M. F. *Eur. J. Org. Chem.* **2007**, 4801–4815. (c) Pirrung, M. C. *J. Am. Chem. Soc.* **1981**, *103*, 82–87. (d) Simmons, P. G. *Quarterly Rev.* **1970**, *1*, 37–68.  
 (13) (a) Lam, E. Y. Y.; Donald, V.; Hammond, G. S. *J. Am. Chem. Soc.* **1967**, *89*, 3482–3487. (b) Wagner, P. J.; David, J. B. *J. Am. Chem. Soc.* **1969**, *91*, 5090–5097.  
 (14) Schmidt, G. M. J. *Pure Appl. Chem.* **1971**, *27*, 647–678.  
 (15) (a) Lem, G.; Nikolas, K. A.; Schuster, D. I.; Ghatlia, N. D.; Turro, N. J. *J. Am. Chem. Soc.* **1993**, *115*, 7009–7010. (b) Fox, M. A.; Cardona, R.; Ranade, A. C. *J. Org. Chem.* **1985**, *50*, 5016–5018.

**Scheme 1.** Photodimerization of 2-Cyclohexenone in the Presence of Host **1**

environment. Larger substrates that could not fit into the channels showed no selectivity. Smaller guests were bound into the cavity but were unreactive, presumably because they were bound in an orientation in which the adjacent enones were  $>4.2$  Å apart or were not in the preferred suprafacial geometry. Together, these studies gave us a clear picture of the nature of the channels within host **1** and the factors that are involved in organizing guests within these channels.

## Results and Discussion

For the reasons above, we were interested in testing if self-assembled host **1** could provide a highly selective confined environment in which to carry out [2+2] cycloaddition reactions. The first example that we examined was the [2+2] cycloaddition of 2-cyclohexenone (Scheme 1). The 2-cyclohexenone was bound into the host structure by exposing the empty host **1** to 2-cyclohexenone vapor, resulting in the formation of a 2:3 host:guest complex.<sup>11</sup> The reaction was carried out in the solid-state by UV-irradiation of the guest filled crystals. The reaction proceeded with excellent selectivity, giving almost exclusively the exo HT product with no starting material left after 24 h. This was impressive for two reasons. First, all of the 2-cyclohexenone could be converted selectively into a single product. Second, all of the product could be removed from the framework via extraction, and the porous crystals recovered and reused without loss of selectivity.

**Goals and Organization of This Study.** On the basis of the above results, we were interested in whether host **1** could be used to carry out [2+2] cycloaddition reactions with small, medium, and large  $\alpha,\beta$ -unsaturated ketones. We were also interested in trying to understand the unique features of our system that facilitated exclusive formation of the exo HT product. In these studies, ten different enones of different size, shape, and symmetry were examined. These enone substrates can be divided into three groups with respect to their molecular volume relative to 2-cyclohexenone. The first substrates are the guests smaller than 2-cyclohexenone **5** (acrylic acid **2**, methylvinylketone **3** (MVK), and 2-cyclopentenone **4**) have calculated molecular volumes ranging from 66 to 80 Å<sup>3</sup>.<sup>16</sup> The second group contains enones that are similar in size ( $\sim 96$  Å<sup>3</sup>) to **5** (3-methyl-2-cyclopentenone **6**, 2-methyl-2-cyclopentenone **7**). Finally, the last set of five substrates are larger than 2-cyclohexenone (mesityl oxide **8**, 2,3-dimethyl-2-cyclopentenone **9**, 3-methyl-2-cyclohexenone **10**, 4,4-dimethyl-2-cyclohexenone **11** and 3,5-dimethyl-2-cyclohexenone **12**). Each set of enones was tested for their ability to be absorbed by the host framework. Next, the conversion of these enones into their photodimer products was examined. The selectivity of their [2+2] cycloaddition reactions within host **1** was studied. Finally, the structure of the bound substrates within host **1** was examined by powder X-ray diffraction and molecular modeling.

(16) The molecular volumes were calculated using Macromodel 5.5: Columbia University: New York, 1996.

**Preparation of Macrocycle 1.** Macrocycle **1** was prepared as previously described and was self-assembled from superheated glacial acetic acid (AcOH), forming the 1:1 inclusion crystals host **1**·AcOH. The AcOH guests were removed by heating at 120 °C for 2 h to yield empty host **1**. The crystalline structure is directed exclusively by the host. Thus, like zeolites, the fidelity of the assembled structure is not changed dramatically by the presence of different guests. Guests can be bound and removed without destroying the self-assembled porous framework. We have demonstrated this with a range of different small molecule guests.<sup>10</sup>

**Scope of the [2+2] Cycloaddition Reaction in the Presence of Host 1.** Each of the 10 different guests (Table 1) was tested for their ability to diffuse into the host framework. Crystals of empty host **1** were sealed in a container in which the headspace was saturated with guest vapor. Guest absorption was followed by <sup>1</sup>H NMR and TGA for 12 h to 14 days, until the system reached an equilibrium, which generally took between 1 and 7 days. Empty host **1** displayed rapid uptake of the small acyclic derivatives **2** and **3** upon vapor treatment and appeared to reach a binding equilibrium (host **1**: enone) within 24 h. Interestingly, the absorption of both the small and medium cyclic enones (**4**–**7**) were kinetically slow, requiring 5–7 days to reach equilibrium. The largest enones that could be absorbed by crystalline host **1** by vapor treatment were **8** and **9** that have molecular volumes of 107 Å<sup>3</sup> and 114 Å<sup>3</sup>, respectively. None of the other large substrates were absorbed even upon prolonged vapor treatment (2 weeks). The uptake of guest by host **1** to form host **1**·guest was monitored by two independent methods: (1) dissolution of a sample in *d*<sub>6</sub>-DMSO and integration of the monomer peaks for host and guest in the <sup>1</sup>H NMR spectra; and (2) heating and measuring the change in weight by TGA upon loss of the included guest.

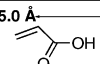
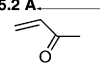
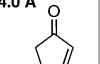
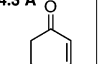
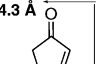
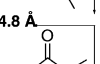
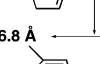
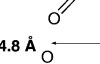
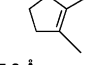
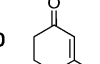
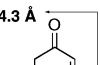
Once loading was complete, the inclusion crystals were removed and immediately subjected to UV-irradiation using a 450 W Hannoveria high-pressure mercury vapor lamp at  $\sim 30$  °C for 24 h. The reaction was monitored at 2, 12, and 24 h by <sup>1</sup>H NMR. The reaction products were removed from the porous framework by washing the crystals with solvent (CH<sub>2</sub>Cl<sub>2</sub> or CDCl<sub>3</sub>). Note that solvent does not dissolve the framework, and the empty host could be efficiently recovered and reused. The conversion observed for each enone and binding ratio (host: guest) is reported in Table 1.

**Conversion and Selectivity Patterns.** Table 1 shows clear trends in terms of the size of the enone with respect to their reactivity within the highly confined environment of host **1**. None of the smaller substrates **2**–**4** reacted in the presence of host **1**, despite the fact that each of these neat substrates undergoes rapid [2+2] cycloaddition reactions. For example, both acrylic acid **2**<sup>17</sup> and MVK **3**<sup>18</sup> form polymeric materials in  $>90\%$  conversion after 12 h of UV-irradiation. These control reactions were carried out by UV-irradiation of the liquid enone. Each of these small guests was bound by host **1** in ratios ranging from 5:2 to 1:2 host:guest. Yet within the complex, they could be subjected to UV-irradiation for up to 48 h without any reaction. After irradiation, the starting materials (**2**–**4**) could

(17) (a) Eastmond, G. C.; Haigh, E.; Taylor, B. *Trans. Faraday Soc.* **1969**, *65*, 2497–2502. (b) Muthukrishnan, S.; Pan, E. H.; Stenzel, M. H.; Barner-Kowollik, C.; Davis, T. P.; Lewis, D.; Barner, L. *Macromolecules* **2007**, *40*, 2978–2980.

(18) White T.; Haward, R. N. *J. Chem. Soc.* **1943**, 25–31.

**Table 1.** Host:Guest Ratios of the Unsaturated Ketones Inclusion Complexes with Crystalline Host **1** and the Control Reactions after 24 h of UV-Irradiation

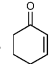
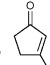
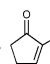
Guest	Volume (Å <sup>3</sup> )	Binding ratio (Host 1:Guest)	Conversion at 24 h (%)	Selectivity to exo HT dimer (%)		
 2	3.0 Å	66	3:2	with host <b>1</b> control	0 > 90 <sup>a</sup>	0 0 <sup>b</sup>
 3	3.0 Å	74	5:2	with host <b>1</b> control	0 > 90 <sup>a</sup>	0 0 <sup>b</sup>
 4	4.2 Å	80	1:2	with host <b>1</b> control	0 > 90 <sup>a</sup>	0 62
 5	4.7 Å	96	2:3	with host <b>1</b> control	100 > 90 <sup>a</sup>	96 35
 6	4.7 Å	97	2:3	with host <b>1</b> control	80 31	98 27
 7	4.2 Å	97	5:2	with host <b>1</b> control	96 27	80 28
 8	3.3 Å	107	5:1	with host <b>1</b> control	0 < 10	0 0
 9	4.7 Å	114	2:3	with host <b>1</b> control	55 3	9 51
 10	4.7 Å	114	not bound	with host <b>1</b> control	0 48	0 54
 11	6.0 Å	130	not bound	with host <b>1</b> control	0 5	0 54
 12	4.8 Å	131	not bound	with host <b>1</b> control	0 48	0 72

<sup>a</sup> Control reactions were monitored at 12 h. <sup>b</sup> Control substrates reacted to give polymers.

be isolated from the host **1** crystals by extraction, and the crystals reused. These results indicate that host **1** safely stores and protects these reactive enones from UV-irradiation. The medium-sized substrates **5–7** selectively form the HT [2+2] dimerization products in good yield. Of the large substrates, host **1** only absorbed guests **8** and **9**. The host **1**·**8** complex did not react upon prolonged UV-irradiation. The host **1**·**9** complex reacted upon UV-irradiation, with 55% of the starting enone converted to a complex mixture of products within 24 h.

Next, we examined the distribution of the photodimeric products of the [2+2] cycloaddition in the presence and absence of host **1**. Table 2 shows the product distribution for enones that selectively formed the exo HT dimer and compared with the control reactions carried out without host **1**. Examination of the reactions in Table 2 reveals the unusually high conversion (100%) and selectivity (96%) for the exo HT dimer initially observed for **5** was also observed for the other medium-sized substrates **6** and **7**. These enones have nearly identical molecular volumes (97 Å<sup>3</sup>) as calculated by MacroModel<sup>16</sup> to that of the original substrate **5** (96 Å<sup>3</sup>); however, they have different

**Table 2.** Selectivity of the [2+2] Cycloaddition after 24 h of UV-Irradiation

medium guest		conversion (%)	selectivity (%)		
			exo HT	exo HH	other isomers
 5	with host <b>1</b>	100	96	3	<1
	control	>90	35	49	8
 6	with host <b>1</b>	80	98	2	<1
	control	31	27	52	16
 7	with host <b>1</b>	95	80	20	0
	control	27	28	72	0

dimensions as estimated by molecular length and width. Substrate **6** (4.2 Å × 4.7 Å) closely matches the dimensions of the original 2-cyclohexenone (4.2 Å × 4.7 Å) and showed similarly high selectivity (98%) and conversion (80%) for the exo HT dimer. Substrate **7** (4.3 Å × 4.8 Å) showed high

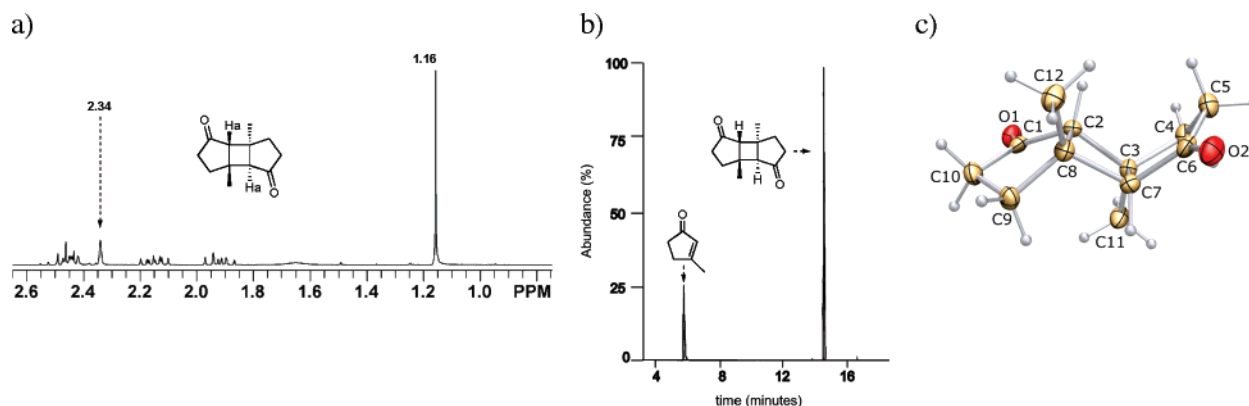
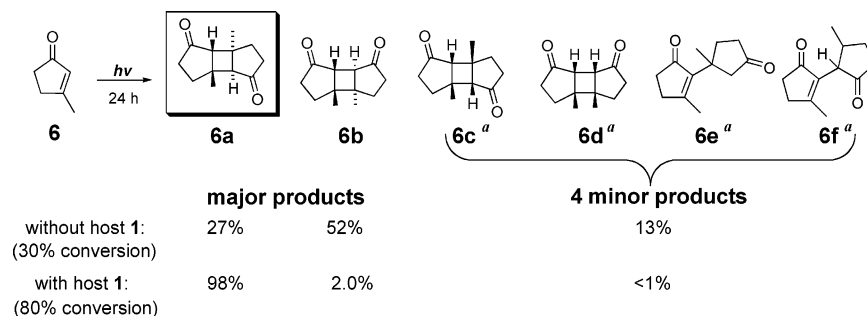


**Figure 2.** Photolysis product of enone **6** with host **1**. (a)  $^1\text{H}$  NMR of the product in  $\text{CDCl}_3$ ; (b) GC–MS of reaction mixture at 24 h. (c) ORTEP X-ray crystal structure of the product.

**Scheme 2.** Photodimerization of **2** in the Presence and Absence of Host **1**



<sup>a</sup> Structures of minor products suggested in literature.

conversion (95%) with slightly lower selectivity (80%) for the exo HT dimer.

The data in Table 2 was measured as exemplified by the procedure for enone **6** shown below. Crystalline host **1**·**6** complex was UV irradiated for 24 h and the product was extracted and characterized without further purification.  $^1\text{H}$  NMR of the crude extract revealed the high selectivity of the reaction, and the spectrum agrees well with the reported data of exo HT product **6a**,<sup>19</sup> displaying only one singlet peak at  $\delta$  1.16 ppm, corresponding to a single methyl group and  $\text{H}_a$  signal at 2.34 ppm (Figure 2a). Slow evaporation of  $\text{CH}_2\text{Cl}_2$  from the extract yielded crystals suitable for the first reported X-ray crystallographic structure of this isomer and confirmed the structure of **6a** as the exo HT dimer (Figure 2c). A more careful analysis by GC–MS (Table 2) established that the cycloaddition of host **1**·**6** is highly selective for **6a** (98%) and shows 80% conversion after 24 h of UV–irradiation (Figure 2c). Only 2% of the HH isomer was observed and less than 1% of one other product. The structures of the other isomers **6c**–**f** (Scheme 2) were previously proposed by Schaffner.<sup>19b</sup> GC–MS suggests that the trace product is **6c** (<1%), as it is less polar and elutes slightly ahead of **6a**, consistent with the assignment of the products in the 2-cyclohexenone series. In comparison, the control reaction of **6** is both kinetically slow, displaying only 31% conversion after 24 h, and is unselective. The control reaction yields a mixture of 6 products each of which displays the expected MW of the dimer 192 g/mol. The ratio of the **6a**

to **6b** is 27:52, in good agreement with literature reports.<sup>20</sup> In summary, the [2+2] photodimerization of **6** proceeded at higher conversion in the presence of host **1** and favors the exo HT product (98%).

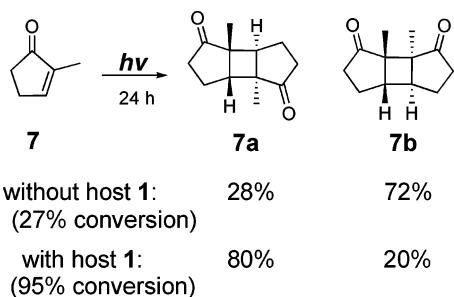
Next, we studied whether the manner by which the enone was loaded into the crystalline host altered the reactivity or selectivity. Enone **6** can also be loaded into the host **1** by soaking the crystals in neat enone.<sup>21</sup> Irradiation of the soaked complex gave a slightly better conversion of enone (87% at 24 h) as compared with the vapor loaded material and correspondingly high selectivity (98%) for **6a** was also observed. The soaking method proved to be a more efficient strategy for guest loading, and we plan to further investigate this loading method for other enones.

Although similar in molecular volume, enone **7** ( $4.3 \times 4.8$  Å) is shorter and wider than **5** and **6**. This difference in shape affects the uptake of **7**, yielding a lower 5:2 host:guest stoichiometry. A rapid [2+2] cycloaddition was observed upon UV–irradiation of the complex and again favored the exo HT isomer (Scheme 3), similar to what is observed in photodimerization of solid-state  $\text{SnCl}_4$  complexes of **7**.<sup>19d</sup> After 24 h,  $^1\text{H}$  NMR analysis showed that only trace amounts of the starting enone **7** remained in the host in addition to the two photolysis products. These were assigned based on the chemical shift of the methyl groups at 1.16 and 0.98 ppm (Figure 3a). Analysis by GC–MS revealed that **7** reacted to yield the photodimers in 95% conversion, forming **7a** with 80% yield and the HH isomer

(19) (a) Mark, G.; Matthaues, H.; Mark, F.; Leitich, J.; Henneberg, D.; Schomburg, G.; Von Wilucki, I.; Polansky, O. E. *Monatsh. Chem.* **1971**, *102*, 37–50. (b) Reinfried, R.; Bellus, D.; Schaffner, K. *Helv. Chim. Acta* **1971**, *54*, 1517–1531. (c) Yvon, K. *Acta Cryst.* **1974**, *30*, 1638–1640. (d) Rao, V. P.; Fech, J. J. *Photochem. Photobiol. A: Chem.* **1992**, *67*, 51–56.

(20) Anklam, E.; Konig, W. A.; Margaretha, P. *Tetrahedron Lett.* **1983**, *24*, 5851–5854.

(21) Host **1** crystals were soaked for 2 h in the liquid enone. The host **1**·**6** complex was then recovered by filtration and air-dried for 5 min. This method of loading produced the same 2:3 host:guest ratio as measured by TGA.

**Scheme 3.** Photodimerization of **7** in the Presence and Absence of Host **1**

**7b** with 20% yield (Figure 3b). Confirmation of the isomeric assignments was provided by crystallographic analysis. Single crystals of the major product formed from slow evaporation of the  $\text{CH}_2\text{Cl}_2$  extract. The crystal structure confirmed the structure of **7a** as the exo-HT dimer (Figure 3c). For comparison, the [2+2] photodimerization reaction of the neat enones was carried out in the absence of host **1**. The control reaction of **7** proceeded markedly slower with only 26.8% conversion by 24 h affording the opposite selectivity. The HH dimer **7b** was the major product (72%) and **7a** (28%) was the minor product. No additional cycloaddition or ring-open products were observed for either the host **1**·**7** complex or the control reactions.

With the larger substrates, only mesityl oxide **8** ( $107 \text{ \AA}^3$ ) and 2,3-dimethyl-2-cyclopentenone **9** ( $114 \text{ \AA}^3$ ) could be loaded into host **1** by vapor treatment and only host **1**·**9** underwent reaction upon UV-irradiation. After 24 h of UV-irradiation, 55% of the starting enone was converted into a complex mixture of 8 isomers, each of which displayed the expected molecular weight of the photodimer (220 g/mol). This conversion was distinctly higher than the control reaction, which showed only 3.3% conversion at 24 h.<sup>22</sup> Mesityl oxide **8** formed a 5:1 complex with host **1**. This complex was stable to prolonged UV-irradiation (48 h). This stability is not surprising given the low reactivity of neat mesityl oxide. The control reaction of neat mesityl oxide displayed <10% conversion after 24 h of UV-irradiation.<sup>22</sup>

The three large substrates (**10–12**) with molecular volumes estimated<sup>16</sup> between 114 and  $130 \text{ \AA}^3$  were not absorbed by host **1** even upon prolonged vapor treatment (>2 weeks), showing that both molecular shape and size (volume) influence binding. To test if these substrates could be absorbed under more forceful conditions, host **1** was soaked in the liquid enones at room temperature for 2 h. After filtration and air-drying, the resulted materials were characterized by  $^1\text{H}$  NMR. Unlike the smaller substrates, which all formed host:guest complexes with reproducible host:guest ratios, these soaked materials did not exhibit steady host:guest ratios and the measured ratios appeared to be dependent on drying time and crystal size. Regardless of the initial host:guest ratio, UV-irradiation of these crystals resulted in photodimerization reactions that were unselective (Table 3). The product distributions were similar to the corresponding control reactions run in the absence of host **1**.<sup>23</sup> Therefore, we assume that these large substrates are not loaded within the channels of host **1** and the unselective reactions observed result

instead from the reaction of disordered enone on the surface of the crystals. This is consistent with the similar distributions of the products for **10**, **11**, and **12** in the presence and absence of host **1** (Table 3).

It is apparent that the size and shape of the guest dramatically affect the absorption of the guest into the host, as well as the efficiency and selectivity of the [2+2] cycloaddition. To understand the origins of these effects, we studied the structure and stoichiometry of the host:guest inclusion complexes, using TGA, PXRD and molecular modeling. For promotion of selective [2+2] cycloaddition, it is likely that the guest enones must (1) be absorbed in significant quantity into the channels of host **1**, forming well-ordered materials; and (2) be oriented in a favorable geometry with the double bonds positioned <4.2  $\text{Å}$  to allow photodimerization.

All of the small- and medium-size substrates (**2–7**) formed stable host **1**·guest complexes with reproducible host: guest ratios at room temperature. Investigation of these complexes by TGA showed that the complexes displayed different temperature stabilities. The literature provides abundant examples of the use of TGA to characterize inclusion complexes.<sup>24</sup> The temperature range at which guest desorption occurs indicates the stability of the complex.<sup>25</sup> The temperature at which half the guest is lost ( $t_{1/2}$ ) provides a measure of complex stability. The desorption of the enones from the inclusion complexes, host **1**·enone was followed by TGA (Figure 4), and the measured weight loss corresponds to the amount of guest bound, allowing calculation of the host:guest binding ratio (Table 1). The complexes with acyclic guests (host **1**·acrylic acid (**2**) and host **1**·MVK (**3**)) displayed a gradual one-step desorption curve from  $\sim 40 \text{ }^\circ\text{C}$  to  $110 \text{ }^\circ\text{C}$  (Figure 4a). For these acyclic guests,  $t_{1/2}$  ranged from 72 to  $81 \text{ }^\circ\text{C}$ . In comparison, the host:guest complexes of the cyclic enones were markedly more stable, displaying no desorption of guest below  $65 \text{ }^\circ\text{C}$ . For example, the host **1**·2-cyclopentenone inclusion complex displayed a sharp, one-step weight loss (26.4%) between  $80 \text{ }^\circ\text{C}$  and  $100 \text{ }^\circ\text{C}$ , with  $t_{1/2} = 93.1 \text{ }^\circ\text{C}$ . The increase in stability of the cyclic enones complexes over the acyclic enone complexes does not appear to correlate with their boiling points but is instead loosely correlated with their molecular dipole moments (Supporting Information). The sharp desorption curves observed for the cyclic enones complexes may indicate that the individual guest molecules are bound more homogeneously within host **1**.

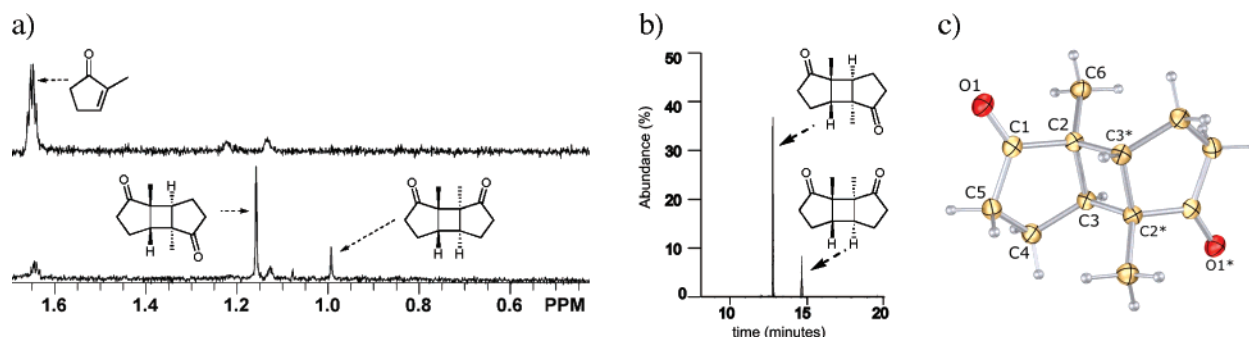
The amount of guest that is absorbed into host **1** varies dramatically over the 10 substrates tested and is associated with size, shape, and polarity of the guest. For example, acrylic acid and MVK have similar sizes ( $\sim 70 \text{ \AA}^3$  volume) and shapes ( $\sim 5.0 \text{ \AA} \times 3.0 \text{ \AA}$ , Table 1). However, the more polar acrylic acid **2** was bound with a higher 3:2 host:guest stoichiometry than with the less polar MVK, which was bound in a 5:2 host:guest stoichiometry. Not only is size and polarity important but shape also appears to be important for efficient guest loading. For example, the absorption of the larger by volume ( $80 \text{ \AA}^3$ ) 2-cyclopentenone **4** ( $4.0 \text{ \AA} \times 4.2 \text{ \AA}$ ) displayed much higher

(22) Yang, N.-C.; Thap, D. M. *J. Org. Chem.* **1967**, *32*, 2462–2465.

(23) (a) Ziffer, H.; Fales, H. M.; Milne, G. W. A.; Field, F. H.; *J. Am. Chem. Soc.* **1970**, *92*, 1597–1600. (b) Schuster, D. I.; Greenberg, M. M.; Nunez, I. M.; Tucker, P. C. *J. Org. Chem.* **1983**, *48*, 2615–2619.

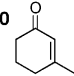
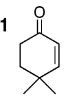
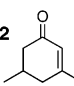
(24) (a) Nassimbeni, L. R.; Su, H. *J. Phys. Org. Chem.* **2000**, *13*, 368–371. (b) Phyoongtamrun, S.; Tashiro, K.; Miyata, M.; Chirachanchaik, S. *J. Phys. Chem. B* **2006**, *110*, 21365–21370. (c) Dey, S.; Pal, K.; Sarkar, S. *Tetrahedron Lett.* **2007**, *48*, 5481–5485.

(25) Nassimbeni, L. R. In *Crystallography of Supramolecular Compounds*; Tsoucaris, G., Atwood, J. L., Lipkowsky, J., Eds.; NATO ASI Series C: Mathematical and Physical Sciences, Vol 480, Kluwer Academic Publishers: Dordrecht, 1995, p 285–305.



**Figure 3.** Photolysis product of enone **7** with host **1**. (a)  $^1\text{H}$  NMR of the product; (b) GC–MS of reaction mixture at 24 h. (c) X-ray crystal structure of the exo head-to-tail product **7a**.

**Table 3.** UV–Irradiation of Host **1** Crystals Soaked in Liquid Enones

Guest		selectivity (%)			
		HT exo	HH exo	HT endo	HH endo
	control	54	24	13	9
	with assembled <b>1</b>	55	33	12	0
	control	54	10	27	9
	with assembled <b>1</b>	53	12	27	7
	control	72	28	0	0
	with assembled <b>1</b>	68	30	1	1

guest loading of 1:2. Given the relatively high loading of **2** and **4**, it is quite surprising that neither of these guests undergo cycloadditions reaction upon UV–irradiation. In comparison host **1**·**5**, in which the guest **5** contains an additional methylene group compared to **4**, displayed a lower loading of 2:3 host:guest and yielded an efficient [2+2] cycloaddition reaction.

To investigate if the inclusion complexes are well-ordered materials, the complexes were ground to a powder and examined by powder X-ray diffraction (PXRD). Figure 5 compares the PXRD patterns of empty host **1** with four host **1**·guest complexes. Inclusion complexes formed from the cyclic enones, 2-cyclohexenone (a), 3-methyl-2-cyclopentenone (b), and 2-cyclopentenone (c) are all highly crystalline, displaying well-defined PXRD patterns that are distinct from each other and from the empty host **1**. This suggests that these guests are well-ordered within the framework of host **1**.<sup>26</sup> When the guests are removed from bulk powder by heating, the empty powder displays a PXRD pattern with peak positions and intensities matching the original empty host **1** (e). In this series, only the host **1**·MVK complex exhibited a PXRD pattern (Figure 5d) similar to the empty host **1**. The PXRD pattern could reflect the lower loading of this guest (1:MVK 5:2) in the complex, or more likely means that the guest is disordered. The low loading of this small guest is probably the reason that no reaction is observed even after 48 h of UV–irradiation. The fact that the

host **1**·MVK complex is unreactive also suggests that the bound MVK does not have much mobility within the solid complex because the neat MVK rapidly polymerizes on UV–irradiation.<sup>18</sup>

Most of the host **1**·guest complexes were well-ordered crystalline materials with distinct PXRD patterns. Unfortunately, it is currently difficult to predict the molecular structure from the PXRD pattern for such complex organic structures. To gain further insight into the structure of the inclusion complexes, we investigated the heptameric assemblies of three of the inclusion complexes: host **1**·**4**, host **1**·**5**, and host **1**·**6** using the molecular modeling program Spartan.<sup>27</sup> The first complex host **1**·**4** is unreactive, whereas the second two complexes undergo selective [2+2]-cycloadditions upon UV–irradiation. These three guests (**4**–**6**) are bound in high host to guest ratios that should facilitate reaction. In addition, each of these three-host guest complexes show well-defined PXRD patterns, indicating that these guests are bound in well-ordered conformations. These two features increase the probability that our molecular models will provide insightful analysis of the structure of these complexes. It is our hypothesis that the selectivity of the reaction is due to the confined environment of the channels.

Assuming that there are only minor structural differences between the filled host **1**·AcOH and the empty host **1**, we can approximate the structure of empty host **1** (Figure 6), using the atomic coordinates from the single-crystal structure of host **1**·AcOH with the guest AcOH omitted.<sup>9</sup> The channel is not straight and alternates back and forth due to alternating edge to face aryl stacking interactions between the macrocycle layers. The channel contains wider openings above and below the plane of the macrocycle alternating with the narrow aperture within the plane of the macrocycle. The distance between the van der Waals surfaces of the carbonyl group (C16A) and phenyl hydrogen (H8) is 4.8 Å and 3.8 Å between phenyl hydrogens (H7 to H23). This model is consistent with the experimental evidence that the empty host **1** does not collapse and displays permanent porosity, showing a type 1 gas adsorption isotherm with CO<sub>2</sub> at 0 °C, with an average pore size of <6.5 Å diameter.<sup>10</sup>

A model of the framework of host **1** containing a single column with seven macrocycles was generated, using the atomic coordinates from host **1**·AcOH. Dynamic simulations on the empty single column of 7 macrocycles in vacuo using Spartan<sup>27</sup> indicated that the major freedom of motion is the tilting of the plane of the aromatics by up to 30°. This type of motion is

(26) (a) Hasegawa, S.; Horike, S.; Matsuda, R.; Furukawa, S.; Mochizuki, K.; Kinoshita, Y.; Kitagawa, S. *J. Am. Chem. Soc.* **2007**, *129*, 2607–2614. (b) Dalrymple, S. A.; Shimizu, K. H. *G. Chem. Comm.* **2006**, 956–959. (c) Tanaka, T.; Tasaki, T.; Aoyama, Y. *J. Am. Chem. Soc.* **2002**, *124*, 12453–12462.

(27) Spartan 04 for Macintosh, v. 1.1.1, 2007, Wavefunction, Inc. Irvine, CA.



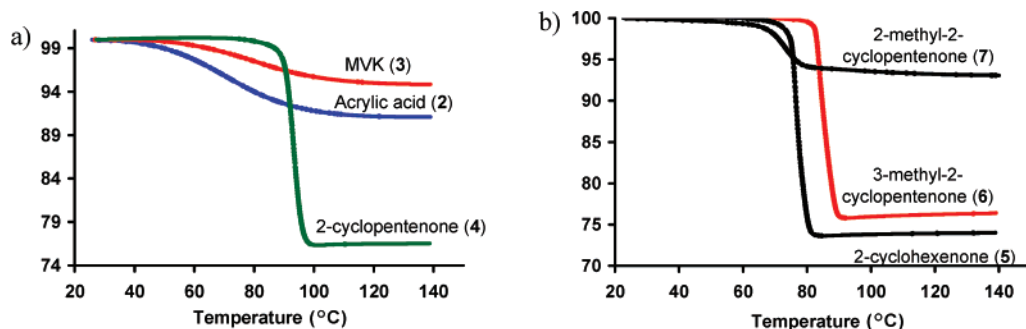


Figure 4. TGA desorption curves for the host **1**·enone complexes with (a) small substrates; (b) medium substrates.

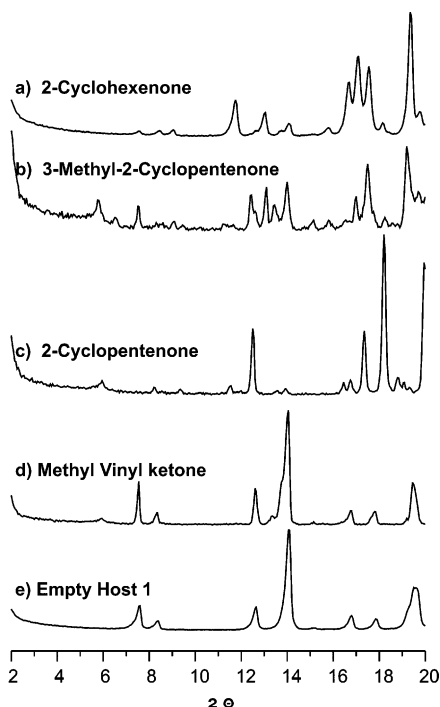


Figure 5. PXRD patterns of (a) host **1**·2-cyclohexenone (**5**), (b) host **1**·3-methyl-2-cyclopentenone (**6**), (c) host **1**·2-cyclopentenone (**4**), (d) host **1**·methylvinylketone (**3**), and (e) the empty host **1**.

likely to be tempered within the crystalline solid. For a first approximation of the filled structure of host **1**·2-cyclohexenone (**5**), the structure of the host was “frozen” so that no movement was allowed in the macrocycle framework. A single guest **5** was added, and the guest was allowed to move to an energy minimum orientation inside the static host structure. Next, a second guest was added, and again with the frozen host, the guests were allowed to move to an energy minimum orientation. The process was repeated until incorporation of further guests caused a guest to be ejected from the ends of the heptamer during minimization. The maximum loading of guests in these short heptamers was 1:1 host:guest, which is a slightly lower loading than the 2:3 host:guest ratio observed experimentally for host **1**·**5**. This might be due to edge effects, which are a result of the small size of the modeled structure. For viewing clarity, the three macrocycles in the center of the modeled structure and two encapsulated 2-cyclohexenone guests are shown in Figure 7a. Monte Carlo searching of the conformer distributions at ground state with Molecular Mechanics (MMFF) suggests that the lowest energy structures have the 2-cyclohexenone guests loaded in an alternating antiparallel geometry with the carbonyl of the enone pointing toward the ureas. The channel

is relatively small compared to the large guest, limiting the number of possible conformations. Enone **5** fits snugly into the cavity, showing a number of close contacts (3–4 Å) between guest and framework atoms. For example, the average distance between the enone oxygen and the urea carbonyl carbons in the heptameric model is 3.7 Å. The alignment of neighboring enone molecules effectively preorganizes the alkenes for a selective [2+2] cycloaddition. Molecular orbital surface calculations using Spartan suggest that the HOMO of one enone and the LUMO of the neighboring enone were aligned in a suprafacial manner with the carbons of the alkene approaching within 3.4 Å, which is well within the optimal distance for the [2+2] photoaddition.<sup>14</sup>

The inclusion complex host **1**·**6** structure (Figure 7b) was constructed via an identical procedure until no further guests could be incorporated into the framework. This yielded a 1:1 host:guest complex, which is a slightly lower loading than the experimentally observed 2:3 host:guest ratio. These molecular mechanics simulations using MMFF suggest that enone **6** is also organized in an alternating antiparallel geometry that favors the formation of the HT dimer, with the enone oxygen pointing generally toward the urea network. In the heptameric model of host **1**·**6**, the enone carbonyl was skewed toward the pocket created by the neighboring aromatic moieties that lie parallel to the column axis. These aryl groups define the pore of the macrocycle and both the ketone from one molecule of **6** and the methyl from the neighboring molecule of **6** fit within this opening. Molecular orbital surface calculations using Spartan predict that the HOMO and the LUMO of the neighboring enones were aligned in a suprafacial manner. Two of the reacting carbons are positioned more closely (~3.5 Å), with the remaining two slightly further apart at 4.2 Å. All were within the required distance for the [2+2] addition to yield the exo HT product.<sup>14</sup> The large guest **6** fills up much of the small cavity and again many close contacts between the guest and host are observed, including close packing of the enone oxygen of the guests within 3–4 Å of the urea nitrogens and carbonyl carbon of the host. These structures indicate that electrostatic and van der Waals interactions play a large role in orienting the guest within the cavity.

An identical procedure was used to construct a model of host **1**·2-cyclopentenone (**4**) complex (Figure 7c). This enone was protected from photoreaction in the presence of host **1**. Again, the simulation did not permit the small host oligomer to be loaded past a 1:1 host:guest ratio; although for this guest, a higher loading (1:2) was observed, experimentally. These molecular mechanics simulations using MMFF suggest that **4** is organized in an alternating antiparallel geometry; however,

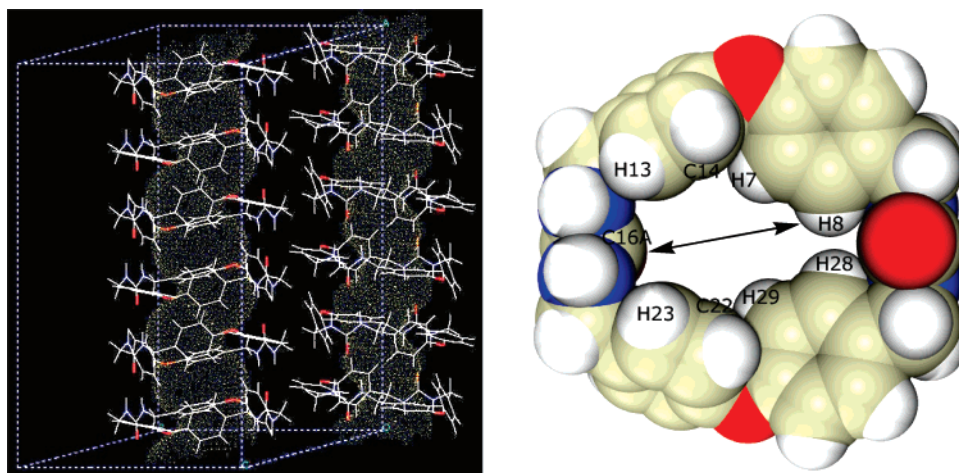


**Figure 6.** Representation of the guest-accessible channels using the single-crystal structure of **1**, with guest AcOH omitted (left). A view of the narrow aperture within the plane of a single macrocycle (right). The distance between the van der Waals surfaces of the carbonyl group (C16A) and phenyl hydrogen (H8) is 4.8 Å and 3.8 Å between phenyl hydrogens (H7 to H23).

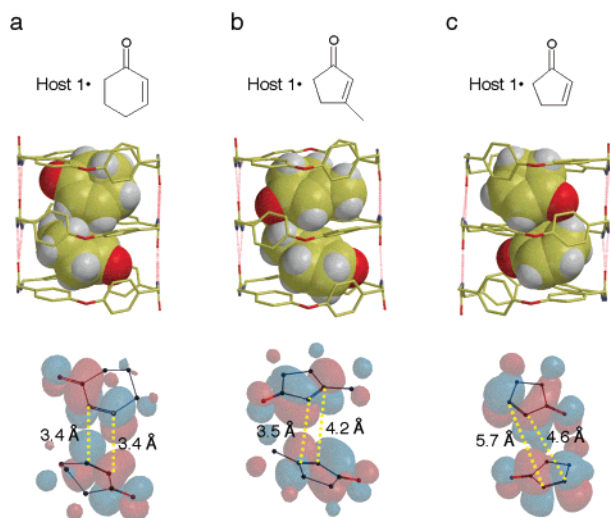


**Figure 7.** Models of the inclusion complexes constructed using Spartan. The hydrogens of the host were omitted for clarity: (a) host **1**·2-cyclohexenone (**5**), (b) host **1**·3-methyl-2-cyclopentenone (**6**), (c) host **1**·2-cyclopentenone (**4**). The HOMO and LUMO of two neighboring enone molecules and the distances between double bonds were calculated using Spartan with MMFF.

the plane of the alkenes no longer approaches each other in the preferred suprafacial orientation. In this case, the two olefins are tilted, nearly 58° in a geometry that is no longer favorable for the [2+2] photocycloaddition reaction. Molecular orbital surface calculations using Spartan show that the HOMO and the LUMO of the neighboring enone were not properly aligned for the reaction.

Taken together, these modeling studies predict that the enones are bound with well-defined geometries within the narrow, zig-zag shaped channels of host **1**. Small changes in the orientation of the enones within the confined environment of the channel greatly influence the outcome of the [2+2] cycloaddition. For example, **4** did not react after 24 h of UV-irradiation; whereas both **5** and **6** displayed selective conversion to their respective HT dimers in high yield. These simple models using a static host scaffold suggest that in the future it may be possible to predict not only which reactants will bind in the channels of the host but also which complexes might show selective

reactions. We are attempting to grow large single crystals of these complexes to elucidate their structures by X-ray diffraction and to compare with the molecular modeling studies.

In summary, host **1** crystals formed by self-assembly of a simple macrocycle provide a robust confined reaction environment for the highly selective [2+2] cycloaddition of 3-methyl-2-cyclopentenone, 2-cyclohexenone, and 2-methyl-2-cyclopentenone, forming their respective exo HT dimers in high conversion. The products are readily extracted from the self-assembled host, and the crystalline host readily recovered and reused. Molecular modeling indicates that origin of this observed selectivity is likely due to the excellent match between the size and shape of these guests to the dimensions of the host channel. The substrates that undergo selective reaction appear to be effectively preorganized within the host channel adopting alternating orientation of neighboring enones, which gives rise to the formation of the observed HT dimer. Substrates of smaller size and molecular volume are also bound within host **1**; however, the host protects these smaller enones from prolonged UV-irradiation. Further examination of one of these smaller complexes, host **1**·2-cyclopentenone by PXRD and molecular modeling indicates that this complex is highly ordered with the host effectively constraining the reactive alkenes in a conformation where the [2+2] cycloaddition is no longer favored. Large substrates either do not form reproducible host:guest complexes or show no difference in selectivity in the presence or absence of host **1**. Presumably, the size and shape of these enones precludes their absorption within the confined channel of host **1**. We are currently examining the use of host **1** as a confined reaction environment for other [2+2] cycloadditions and unimolecular rearrangements and will report on these in due course.

## Experimental Section

**General Information.** All chemicals were obtained from Sigma-Aldrich Chemical Company and used without further purification. The enone guests were purchased as reagent grade.

**Preparation of Host 1.** Macrocycle **1** was synthesized and crystallized as previously described.<sup>9</sup> Ground or unground crystals of **1**·AcOH were evacuated by heating at 120 °C to form the empty host **1**, which was cooled in a desiccator to room temperature. The loading of enone guests was carried out in the dark in vessels covered with aluminum foil.

**Loading of Guests into Host 1.** Crystals of host **1** (116 mg) were added to a 20-mL scintillation vial and exposed to guest vapor (10 g) in a sealed vessel for between 12 h and 2 weeks. Small amounts (1–2 mg) of the solid material were taken to check the  $^1\text{H}$  NMR every 24 h until the system reached an equilibrium. Loading of the guest vapor was time-dependent and appeared to reach a maximum at 5–7 days for the cyclic enones. Loading of acyclic substrates was more rapid, reaching a maximum in 24 h. The host:guest binding ratio was determined by both TGA and  $^1\text{H}$  NMR.

**NMR Studies.** Samples of host **1** were transferred directly into an NMR tube and dissolved in 1 mL of  $d_6$ -DMSO solvent. The NMR tube was sonicated until all the material was dissolved. The NMR spectra were recorded using a 300-MHz Mercury Varian NMR spectrometer. The macrocycle:guest ratios were determined by the  $^1\text{H}$  NMR integration. Delay times were optimized for integration.

**PXRD Studies.** X-ray powder diffraction data were collected either on a Rigaku DMAX-2100 or Rigaku DMAX-2200 powder X-ray diffractometer using  $\text{Cu K}\alpha_1$  radiation with graphite monochromator. Data were collected at an increment of  $0.05^\circ$  and an exposure time of 5 s/step in the angular range  $2\text{--}20^\circ 2\theta$  at ambient temperature. The GC–MS spectra were obtained with Micromass VG70S magnetic sector mass spectrometer, Column: Restek RTX-5, 30 m  $\times$  0.25 mm, 0.25- $\mu\text{m}$  film thickness.

**TGA Studies.** Guest desorption studies were carried out on 5–10 mg of empty host **1** after equilibration with each guest in the vapor chamber. Thermogravimetric analyses (TGA) were performed using a TA Instruments Q600 simultaneous DTA-TGA. All samples were analyzed, using the same method with a heating rate of  $4^\circ\text{C}/\text{min}$  from 25 to  $140^\circ\text{C}$  under helium. Upon completion, each sample was recollected for the next absorption/desorption cycle.

**Photoreaction.** Photocycloaddition of enones were carried out, using a Hanovia medium-pressure 450-W mercury arc lamp cooled in a

borosilicate immersion well, and the entire apparatus was placed in a UV shielded and refrigerated reaction chamber. The starting temperature was  $0^\circ\text{C}$ , and the final temperature did not increase above  $30^\circ\text{C}$  after 24 h of irradiation. A 20 mL scintillation vial containing 50 mg host–guest complex or a 4 mL glass vial containing 100 mg neat enone liquid were placed in proximity to the lamp (3–5 cm) and irradiated for 24 h. After the irradiation, small samples of host–guest complex and the control were studied by  $^1\text{H}$  NMR. The control reactions were dissolved directly in  $\text{CDCl}_3$  and the solutions were also analyzed GC–MS. For the complex, crystals were either dissolved in  $d_6$ -DMSO or shaken with 1 mL  $\text{CDCl}_3$  for 1 h. The empty host **1** was recovered by filtration and washed with  $\text{CDCl}_3$  ( $2 \times 0.5$  mL). The recovered host **1** was dissolved in  $d_6$ -DMSO for  $^1\text{H}$  NMR analysis. There was no detectable enone and dimer product in the washed host. The  $\text{CDCl}_3$  filtrate was analyzed by  $^1\text{H}$  NMR and GC–MS. Single crystals of the dimerization products were obtained upon slow evaporation from this solution and used for X-ray crystal structure analysis.

**Acknowledgment.** This work was supported by the NSF (CHE-071817), by the Petroleum Research Fund (44682), and by a grant from the University of South Carolina, Office of Research and Health Sciences Research Funding Program.

**Supporting Information Available:** Experimental details, GC/MS data, and full characterization of the major cycloaddition products including crystallographic information files. This material is available free of charge via the Internet at <http://pubs.acs.org>.

JA076001+